Stem Cell Rev and Rep (2015) 11:309–321
DOI 10.1007/s12015-014-9573-5

Ovariectomized Rats with Established Osteopenia have Diminished Mesenchymal Stem Cells in the Bone Marrow and Impaired Homing, Osteoinduction and Bone Regeneration at the Fracture Site

Deepshikha Tewari · Mohd Parvez Khan · Nitin Sagar · Shyamsundar P. China · Atul K. Singh · Subhash C. Kheruka · Sukanta Barai · Mahesh C. Tewari · Geet K. Nagar · Achchhe L. Vishwakarma · Omeje E. Ogechukwu · Jayesh R. Bellare · Sanjay Gambhir · Naibedya Chattopadhyay

Published online: 30 November 2014

Abstract We investigated deleterious changes that take place in mesenchymal stem cells (MSC) and its fracture healing competence in ovariectomy (Ovx)-induced osteopenia. MSC from bone marrow (BM) of ovary intact (control) and Ovx rats was isolated. ^{99m}Tc-HMPAO (Technitium hexamethylpropylene amine oxime) labeled MSC was systemically transplanted to rats and fracture tropism assessed by SPECT/CT. PKH26 labeled MSC (PKH26-MSC) was bound in scaffold and applied to fracture site (drill-hole in femur metaphysis). Osteoinduction was quantified by calcein binding and microcomputed tomography. Estrogen receptor (ER) antagonist, fulvestrant was used to determine ER dependence of osteo-induction by MSC. BM-MSC number was strikingly reduced and doubling time increased in Ovx rats compared to control. SPECT/CT showed reduced localization of ^{99m}Tc-HMPAO labeled MSC to the fracture site, 3 h post-transplantation in Ovx rats as compared with controls. Post-transplantation, Ovx MSC labeled with PKH26 (Ovx PKH26-MSC) localized less to fracture site than control PKH26-MSC. Transplantation of either control or Ovx MSC enhanced calcein binding and bone volume at the callus of control rats over placebo group however Ovx MSC had lower efficacy than control MSC. Fulvestrant blocked osteoinduction by control MSC. When scaffold bound MSC was applied to fracture, osteoinduction by Ovx PKH26-MSC was less than control PKH26-MSC. In Ovx rats, control MSC/E2 treatment but not Ovx MSC showed osteoinduction. Regenerated bone was irregularly deposited in Ovx MSC group. In conclusion, Ovx is associated with diminished BM-MSC number and its growth, and Ovx MSC displays impaired engraftment to fracture and osteoinduction besides disordered bone regeneration.

Keywords Fracture healing · Animal imaging · Transplantation · Estrogen deficiency · Femur metaphysis · Cell migration

D. Tewari · M. P. Khan · S. P. China · M. C. Tewari · G. K. Nagar · O. E. Ogechukwu · N. Chattopadhyay (✉)
Division of Endocrinology and Centre for Research in Anabolic Skeletal Targets in Health and Illness (ASTHI), CSIR-Central Drug Research Institute, B.S. 10/1, Sector-10, Jankipuram Extension, Lucknow, India
e-mail: n_chattopadhyay@cdri.res.in

N. Sagar · A. K. Singh · J. R. Bellare
Departments of Chemical Engineering, CRNTS and Biosciences and Bioengineering, Indian Institute of Technology-Bombay, Powai, Mumbai 400076, India

S. C. Kheruka · S. Barai · S. Gambhir
Department of Nuclear Medicine, Sanjay Gandhi Post Graduate Institute of Medical Sciences, Raebareli Road, Lucknow 226014, UP, India

A. L. Vishwakarma
Sophisticated and Analytical Instrumentations Facility, CSIR- Central Drug Research Institute, B.S. 10/1, Sector-10, Jankipuram Extension, Lucknow, India

Introduction

Osteoporosis is associated with a higher fracture risk in post-menopausal women with a diminished capacity of bone to heal due to estrogen (E2) deficiency [1] which causes significant morbidity. Osteopenia could also occur in females of reproductive age having low levels of circulating E2 due to a disease called hypothalamic amenorrhea (HA) [2]. Ovariectomy

(Ovx) in females performed at an age younger than the average age of the natural menopause due to other clinical causes are at higher risk of fracture due to osteopenia [3]. In the bone marrow (BM), a decline in the availability of osteogenic prescursor cells [4] may be associated with impaired fracture healing in E2-deprived individuals.

Currently, recombinant human bone morphogenetic protein-2 (BMP-2) and BMP-7 are approved for spinal fusion surgery and treatment of recalcitrant tibial fractures, respectively [5]. Recently, recombinant platelet-derived growth factor-BB has obtained U.S. FDA approval for the treatment of accelerated periodontal regeneration [6]. Development of various forms of grafts, aimed at enhancing bone regeneration, whether injected or applied in an open technique could facilitate osteoinduction and lead to osteogenesis [7–9]. However, these approaches are associated with significant surgical morbidity particularly in individuals with osteopenia. Presently, there is no therapy available to promote fracture healing in osteopenic individuals.

Systemic administration of bone marrow-derived mesenchymal stem cells (MSC) may represent a novel nonunion therapy with no surgical morbidity especially in E2-deprived individuals. Clinical studies have shown that systemic transplantation of MSC is safe and well tolerated [10] and is effective in the treatment of osteogenesis imperfecta [11]. Recent evidence suggests that MSC are mobilized from peripheral sites in patients bearing acute fractures and are detectable in the circulation [12], suggesting a physiological role of MSC mobilization from distant source and recruitment to the site of fracture. Animal studies have demonstrated that systemically infused MSC migrate to the site of fracture and engraft into the site at greater efficiency than locally transplanted cells [13, 14]. However, not much is known about MSC behavior per se under osteopenic condition and their fracture healing characteristics.

Loss of cancellous metaphyseal bones are commonly observed in postmenopausal individuals [15, 16]. Females with a history of HA have low trabecular bone densities as compared to age-matched controls, even after recurrence of normal menstruation [2]. Bone loss in postmenopausal women also occurs in the diaphyseal bone, although to a lesser extent [17]. The process of periosteal apposition continues to preserve the mechanical strength of cortical bone [18]. Therefore, long bones are more susceptible to fractures at the metaphysis rather than at the diaphysis. In laboratory mammals with osteopenia, the fracture healing process is delayed and poor in quality [19, 20]. In women, postmenopausal osteoporosis negatively influences the fracture healing process, and the recovery of functional competence is delayed [21, 22]. Reduced stromal/osteoprogenitor population in the BM of Ovx animals has been reported. Available studies also indicate that E2 deficiency diminishes MSC renewability and osteogenic differentiation of BM-MSC which could lead to poor bone regeneration upon systemic transplantation [23, 24]. However, there are no systematic studies assessing the impact of osteopenia on MSC functions including, the ability to migrate at the fracture site (homing) and induction of bone regeneration.

We used Ovx rat model to evaluate therapeutic efficacy of MSC in long term E2 deprived condition for the present study. As the prevalence of E2 deprived fractures in the long bones of humans are located at the metaphysis, we made drill-hole wound of femur metaphysis to study osseous wound/fracture healing. We first studied the impact of E2 deprived condition induced by prolonged Ovx on the number and growth ability of BM-MSC. Next, we made comparisons between MSC isolated from ovary intact and Ovx rats on a) migration to fracture site and b) osteoinduction and the pattern of bone regeneration in E2-replete rats. Osteoinduction by MSC isolated from ovary intact and Ovx rats were also studied.

Material and Methods

Reagents and Chemicals

Cell culture media, MSC qualified FBS and supplements were purchased from Invitrogen (Carlsbad, CA). All fine chemicals including 17β-estradiol (E2), fulvestrant and calcein were purchase from Sigma-Aldrich (St. Louis, MO).

Animals

All animal experimental procedures were prior approved (Institutional Animal Ethics Committee approval number (CDRI/IAEC/2012/17) and conducted as per the guide lines laid by the Committee for the Purpose of Control and Supervision of Experiments on Animals (CPCSEA 34/199). Female Sprague Dawley (SD) rats (200±20 g) were used throughout the study. Rats were obtained from the National Laboratory Animal Centre, CSIR-CDRI and were kept in a 12 h light–dark cycle, with controlled temperature (22–24 °C) and humidity (50–60 %) and free access to standard rodent food and water.

Isolation and Expansion of MSC

For MSC isolation, BM was harvested and pooled by flushing the tibias and femurs of healthy and Ovx female rats (n=18 for each group) and cultured in α-MEM supplemented with 10 % FBS, glutamax (2 mg/ml) and 1 % penicillin-streptomycin. After 48 h, adherent cells were expanded. Magnet-associated cell sorting (MACS) was done at passage 2 as described before [25]. In brief, we used a kit-based sorting (BD, New Jersey, USA) in which cells were first tagged with biotinylated CD90 and CD54 antibodies, then mixed with IMag streptavidin particles and finally sorted by magnet. $CD90^{+}$

and $CD54^+$ cells were cultured. Cells of the passage 3 were used throughout the present study. For determination of doubling time of MSC isolated form healthy and Ovx rats, 4×10^4 cells/well were seeded in 6-well plates in triplicate. After 72 h, cells were harvested, stained with trypan blue and counted by hemocytometer (Hausser Scientific, Horsham, PA, USA). Doubling time was calculated by a method described before [26].

Flow Cytometry

MACS purified cells at passage 3 (P3) were analyzed for MSC surface antigen by flow cytometry for which cells were first incubated for 30 min at room temperature (RT) with various primary antibodies including, FITC-conjugated CD90 (Abcam, MA, USA), purified-CD54 (BD), purified-CD29 (Abcam), purified-CD73 (BD), PE-conjugated CD45 (Abcam) and MHC class II (Abcam). Cells were washed and CD54, CD29 and CD73 tubes were incubated with secondary antibody, IgG FITC (Abcam) for 45 min at RT. Cells were fixed in 4 % paraformaldehyde. Labeled cells were then analyzed in FACS Calibur (Becton and Dickinson).

MSC Differentiation to Osteoblasts and Adipocytes

MSC (1×10^4 cells/well) were plated in 6-well plates and cultured in complete medium. At 90 % confluence, medium was changed to osteoblast differentiation medium (10nM dexamethasone, 10 mM β-glygerophosphate and 50 μg/ml ascorbic acid) and adipocyte differentiation medium (0.5 mM IBMX, 100 μM indomethacin, 10 μg/ml insulin and 1 μM dexamethasone) for 21 days with a change of medium every 48 h. Deposition of mineral (nascent calcium) was determined by staining with Alizarin red-S (40 mM, pH 4.5). The stain was extracted using 10 % (v/v) acetic acid for 30 min at RT. Cells were scraped and collected in 1.5 ml tube. After brief bursts of vortexing, the slurry was overlaid with 500 μl mineral oil and heated to 80 °C for 10 min and transferred to ice for 5 min. The slurry was then centrifuged at 20,000 g for 15 min and supernatant was collected. Then 200 μl of 10 % (v/v) ammonium hydroxide was added to neutralize the pH. Optical density (OD) of the extracted dye was recorded at 405 nm [27]. Nodules area was calculated from captured photomicrographs using image proplus analysis 6.1 software. Adipogenesis was assessed for the presence of fat droplets visualized by Oil red-O stain. In brief, the differentiated cells were fixed in 4 % paraformaldehyde w/v for 20 min. After washing with PBS, cells were stained with 0.34 % Oil red-O in 60 % isopropanol for 15 min. Cells were washed with PBS and dye was extracted with 80 % isopropanol. OD of the extracted dye was recorded at 520 nm [28]. Data obtained from both dye extraction methods are presented as fold change from control MSC after protein normalization.

Ovx and Drill-Hole Injury of Femur Metaphysis

Rats were bilaterally Ovx and left for 13 weeks to develop E2 deprived osteopenia [29]. A drill-hole injury was created by inserting a drill bit with a diameter of 0.8 mm in the femur metaphysis region following our previously described protocol with minor modification with respect to drill-hole spot [30]. On the fourteenth day, rats were killed and bones appropriately preserved for histology, histomorphometry and micro-computed tomography (μCT) following our previously described methods [31]. Twenty-four hours before killing, all animals received calcein (20 mg/kg) by intraperitonial route. On the fourteenth day, the rats were killed by overdose anesthetization for the collection of femurs. The bones were kept in 70 % isopropanol and embedded in anacrylic material. Then, 50 μm sections were made from the bones using Isomet-SlowSpeedBoneCutter

(Buehler, LakeBluff,IL), followed by imaging using confocal microscope (LSM 510 Meta, Carl Zeiss, Inc., Thornwood, NY) with appropriate filters. The intensity of calcein binding was calculated using Carl Zeiss AM 4.2 image-analysis software.

Cell Labeling with ^{99m}Tc-HMPAO

To quantify migration of MSC to the fracture site by dual head SPECT/CT (Siemens, Erlangen), the cells were labelled with ^{99m}Tc-HMPAO a lipophilic WBC radio-labelling linker (Polatom, Poland) following previously described protocol and guidelines [32]. For this fractured female rats (cont rats; n=9) were equally divided in 3 groups viz. i) cont rats +1 million MSC labeled with ^{99m}Tc-HMPAO, ii) cont rats +2 million MSC labeled with ^{99m}Tc-HMPAO, iii) cont rats +4 million MSC labeled with ^{99m}Tc-HMPAO. Labelling efficiency (% radio counts in cell pellet) and viability by tryphan blue exclusion tests were found to be 35–40 % and 98 % respectively. Before labelling, MSC were washed twice with PBS. To 1×10^6 MSC suspended in 1 ml PBS, ^{99m}Tc (370–555 MBq) having physical half-life of 6.02 h and γ energy, 140±10 % KeV was added and incubated for 30 min at R.T. Unbound radioactivity was washed and labeled MSC were suspended in 1 ml saline for injection through tail vein. After 3 h, image of in vivo bio-distribution of ^{99m}Tc-MSC was acquired for 5 min using dual head SPECT/CT gamma camera and quantification of bio-distributed radio-labeled MSC at fracture site was derived. The radioactive count sensitivity of gamma camera was 201,429 counts/mCi/min (cpm) and the resolution of imaging was 8.15 mm.

The method for quantification of MSC involved conversion of radioactive counts at fracture site to number of cells. Region of interests (ROI) was drawn over the whole rat and the fracture site on a 3 h SPECT-CT image acquired for 5 min and radioactive counts recorded as cpm/mm^2 at 140±10 %

KeV energy window of technetium. Three-hour decay correction was applied to ROI counts. 'Net injected radioactive counts' was obtained by subtracting post injection syringe counts from the pre-injection syringe counts in a gamma well counter (Capintec CRC 15 beta). The 'net injected radioactive counts' were taken as representing 1-, 2- and 4 million MSC in different experiments. The proportion of 'radioactive counts on fracture site ROI' compared with 'net injected radioactive counts' was used to derive proportion of MSC localization to fracture site.

MSC Therapy in Fractured Rats

From BM of Ovx rats and sham operated (ovary intact, control) rats, MSC was isolated as described above. For fracture healing studies with control (cont) MSC (MSC isolated from BM of rats with intact ovary) and Ovx MSC (MSC isolated from BM of Ovx rats), drill-hole injury was created in normal female (cont rats) and randomised in the following groups according to their treatment; i) Placebo, ii) cont MSC, iii) Ovx MSC, iv) fulvestrant (30 mg/kg/d; s.c) + cont MSC. Further fracture healing studies with cont MSC and Ovx MSC, drill-hole injury was created in Ovx rats and randomised in the following groups according to their treatment i) Placebo, ii) cont MSC, iii) Ovx MSC, iv) E2 (60 μg/kg/d: s.c). All above group consisted of 10 rats. Before administration of a total number of 1×10^6 cont MSC or Ovx MSC per animal via tail vein, a red fluorescent dye PKH26 was used to label MSC using a Cell Linker Kit (Sigma-Aldrich) by following manufacturer's protocol. Briefly, 1×10^6 cells were harvested by trypsinization, and resuspended in a diluent buffer containing 2×10^{-6} M PKH26 staining reagent was added. The cells were incubated at RT for 5 min and the reaction was stopped by adding equal volume of 10 % FBS. Labeled cells were recovered by centrifugation and resuspended in normal saline. Labeling efficiency was >95 % and the cell viability was >97 %, as assessed by fluorescent microscopy and trypan blue exclusion, respectively.

Micro-Computed Tomography (μCT)

μCT determination of excised bones was analyzed using Sky Scan 1076 μCT scanner (Aartselaar, Belgium). Bone were cleaned of soft tissue and scanned using a X-ray source of 70 kV, 100 mA with a pixel size of 18 μm. Reconstruction was carried out using a modified Feldkamp 188 algorithm using Sky Scan Nrecon software (Sky Scan, Ltd., Belgium). Callus bone was captured by drawing ellipsoid contour with CT analyzer software. Microarchitectural parameters including, bone volume fraction (BV/TV), trabecular thickness (Tb.Th), trabecular separation (Tb.Sp), trabecular number (Tb.N) and structure model index (SMI) were quantified as described before [33, 34]

Loading of MSC with 3D Scaffold at Fractured Site

To study the therapeutic effect of cont MSC and Ovx MSC in equal number with 3D scaffold at fractured site in female rats was evaluated. A 3-D nano-hydroxyapatite/gelatin/carboxymethyl chitin (n-HA/gel/CMC) scaffold constructs were prepared by solvent casting method combined with glutaraldehyde vapour crosslinking and freeze drying method as described before [35, 36]. The scaffolds were removed from the sterile patches and wetted with blood that oozed out from the incision during surgery. This allowed the scaffold to become compliant. The n-HA-gel-CMC scaffold construct loaded with 2×10^4 cont MSC or Ovx MSC was then placed into the fractured site of female rats, that were equally divided in 3 groups viz. i) Placebo (P) + scaffold (S; n=6), ii) cont MSC + S (n=12), iii) Ovx MSC + S (n=12). Rat (n=6) of group ii) and iii) were sacrificed on day 3 for the evaluation of PKH 26 labeled MSC intensity. On day 14, rats of all 3 groups (n=6 of each group) were sacrificed, whereas twenty-four hours before killing, all animals received calcein (20 mg/kg) by intraperitonial route. μCT and confocal imaging for calcein intensity was performed in all these groups.

Statistical Analysis

Data are expressed as mean ± S.E.M. The significant difference was analyzed by student's t-test or one-way ANOVA followed by post hoc Newman Keuls multiple comparison test of significance using GraphPad Prism 5 software. Qualitative observations have been represented following assessments made by two researchers blinded to the experimental designs.

Results

Assessment of Trabecular Osteopenia After Ovx

Sham operated rats (ovaries intact) served as control for intact trabeculae. Thirteen-week post-Ovx, BMD, BV/TV, Tb.N and Tb.Th were significantly reduced while Tb.Sp increased compared to control (Table 1). Furthermore, in previous reports, we showed that the trabecular osteopenia thus induced had resulted in decreased compressive strength [29, 37]. Together, from our present and previous data it appeared that 13 weeks post-Ovx induced significant trabecular osteopenia in rats.

Purification and Characterization of BM-MSC

Bone marrow cells of tibia and femur were subjected to MACS, cultured and at the second passage MSC was purified by flow cytometry (passage 3). At this stage, cells exhibited the expression of MSC markers including CD29 (99.47 %),

Table 1 Assessment of induction of osteopenia in Ovx rats

	BV/TV (%)	Tb. N (1/mm)	Tb. Sp (mm)	Tb. Th (mm)	BMD (gmHA/cm^3)
Sham	51.6±3.4	3.6±0.26	0.42±0.05	0.15±0.003	1.04±0.07
Ovx	42.2±4.14**	2.1±0.29***	0.59±0.04**	0.16±0.008	0.689±0.05**

Bone parameters at femur epiphysis are shown in sham and Ovx (13 weeks post-Ovx); data represent mean ± SEM; n=10 rats/group

BV/TV (%) bone volume/trabecular volume, *Tb.N* trabecular number, *Tb.Sp* trabecular spacing, *Tb. Th* trabecular thickness, *BMD* bone mineral density

**p<0.01, ***p<0.001vs. sham

CD54 (95.46 %), CD73 (99.22 %) and CD90 (99.82 %), but negative (less than 1 %) for hematopoietic markers CD45 and MHC class II (Fig. 1), suggesting an overall >99 % purity of MSC.

BM-MSC Number and Proliferation

In a femur drill-hole fracture model, we have previously shown that bone deposition at the callus of Ovx (osteopenic) rats is significantly lower than that in ovary intact rats [33]. We speculated that E2 deficiency could alter the physiology of BM-MSC. First, we assessed the relative abundance of BM-MSC between the control and Ovx rats. CD90+ and CD54+ expressing MSC isolated by MACS varied from 0.1 to 0.01 % of the total BM cells in control rats (data not shown). Determination of relative abundance showed that Ovx rats had strikingly reduced BM-MSC than the control (p<0.01) (Table 2).

Comparison of Growth and Differentiation of MSC

We next determined the doubling time of MSC derived from the control and Ovx groups. Table 2 showed that doubling time increased by 68–70 % in BM-MSC from Ovx rats than that from the control (p<0.05). Osteogenic differentiation of Ovx MSC was lower than control MSC (p<0.001) (Fig. 2a). By contrast, adipogenic differentiation of Ovx MSC assessed by oil-red O staining was higher than the control MSC (p<0.001) (Fig. 2b). Furthermore, control MSC treated with E2 had robust increase in osteogenic differentiation but E2 had no such effect on Ovx MSC (Fig. 2c).

MSC Migration to the Fractured Site

After confirming substantial osteopenia induction by Ovx and demonstrating that BM-MSC had reduced growth rate, we next studied the in vivo dynamic trafficking and homing in response to femur metaphysis fracture cue by Ovx MSC in comparison to control MSC. First, we determined the migration of systemically transplanted control MSC to fractured site in cont rats. Increasing number of ^{99m}Tc-HMPAO labelled MSC (1-, 2- and 4×10^6 cells) was transplanted to rats 24 h after drill-hole was made and SPECT/CT was performed. An early and substantial lung trapping after transplantation was observed in all animals. Three-hour post-transplantation, the fracture bearing femur detected significant radioactivity

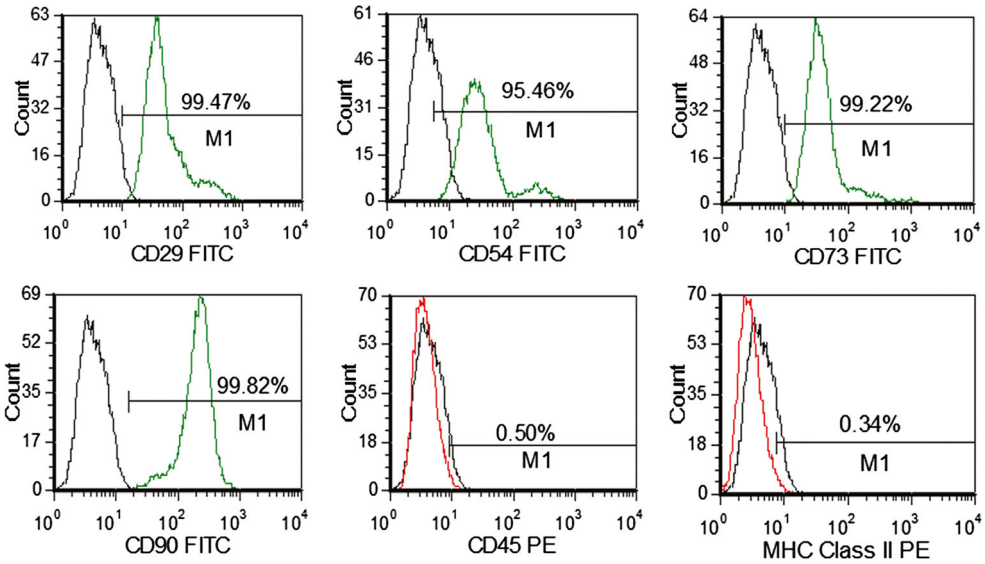

Fig. 1 Characterization of BM-MSC by MACS. Flow cytometry analysis showed the expression of MSC positive markers such as CD90, CD29, CD73, CD54 and less than 1 % negative markers as CD45 and MHC class II

Table 2 BM-MSC number and doubling time

	Control	Ovx
BM $CD90^+$ and $CD54^+$ cells after MACS (in millions)	0.06±0.007	0.002±0.001**
Doubling time (hours)	73.64±6.0	123.43±7.6*

Data represented as mean ± SEM, (n=3)

*p<0.05, **p<0.01 vs. control

(Fig. 3). Percentage of MSC localized to the fracture site was dose-dependently decreased (Fig. 4a), although the number of labeled cells at the site that was calculated from the radioactivity counts was similar between different input numbers, suggesting that saturation was attained with 1×10^6 cells (Table 3). In comparison to control MSC, transplantation of equal number of Ovx MSC resulted in the detection of only 1/4th radioactivity at the fracture site (Fig. 4b).

We used PKH26 (red fluorescent) labeled MSC to monitor their localization to the fracture site and bone regeneration, because ^{99m}Tc has a half-life of 6 h and gamma camera sensitivity did not allow radio-detection of cells beyond four

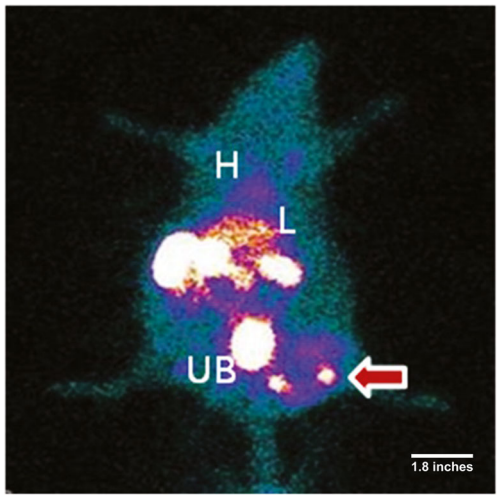

Fig. 3 Representative image of in vivo bio-distribution of cont ^{99m} Tc-HMPAO-labeled MSC in an ovary intact adult female rat with fracture at femur metaphysis acquired 3 h after injection using a dual head SPECT/CT gamma camera. H: Heart; L: Lung; UB: Urinary Bladder; Red Arrow: fracture site

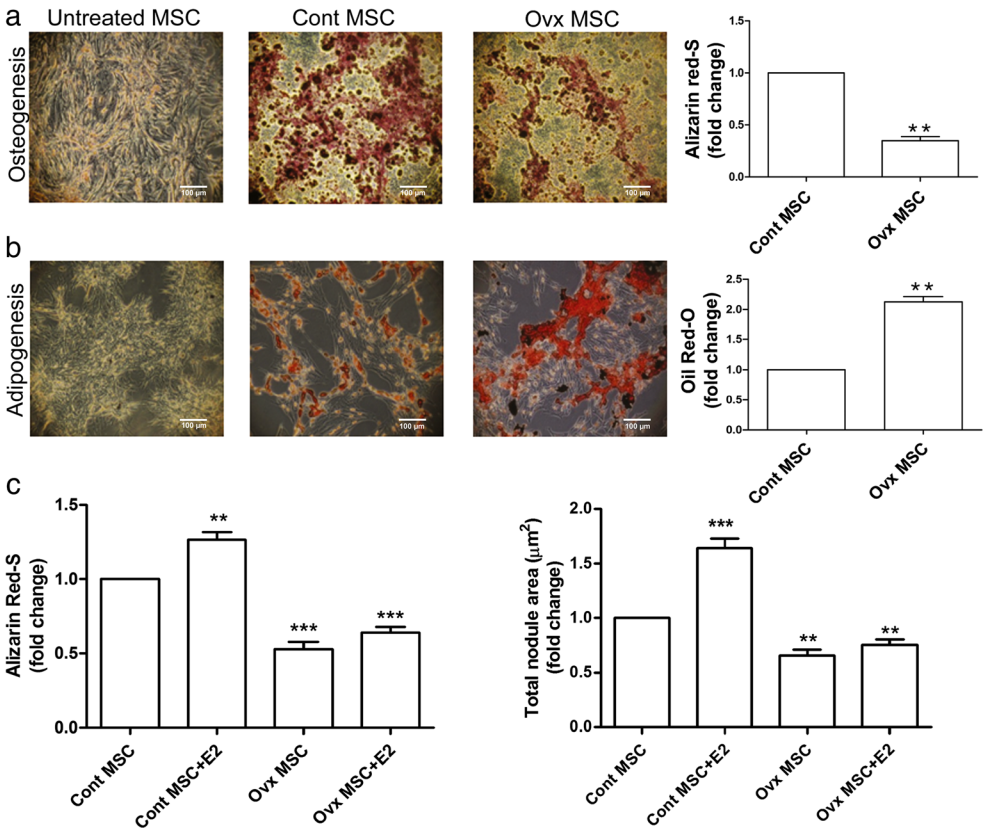

Fig. 2 Differentiation of BM-MSC to osteoblasts and adipocytes in response to different stimuli. (**a**) Representative photomicrograph showing alizarin red-S stain of MSC cultures in osteogenic medium. Dye extraction followed by optical density (OD) determination showed reduced alizarin staining in Ovx MSC compared with control (cont) MSC. (**b**) Representative photomicrograph showing oil red-O stain of BM-MSC cultures in adipogenic medium. Dye extraction followed by OD determination showed increased oil red-O staining in Ovx MSC compared with control MSC. (**c**) E2 (10 nM) stimulated osteogenic differentiation of cont MSC but not Ovx MSC. *Left* panel, quantification of alizarin red-S extracted stain and right panel, total nodule area quantified from the alizarin red-S positive fields. Values are expressed as mean ± SE (n=3); **p<0.01, ***p<0.001

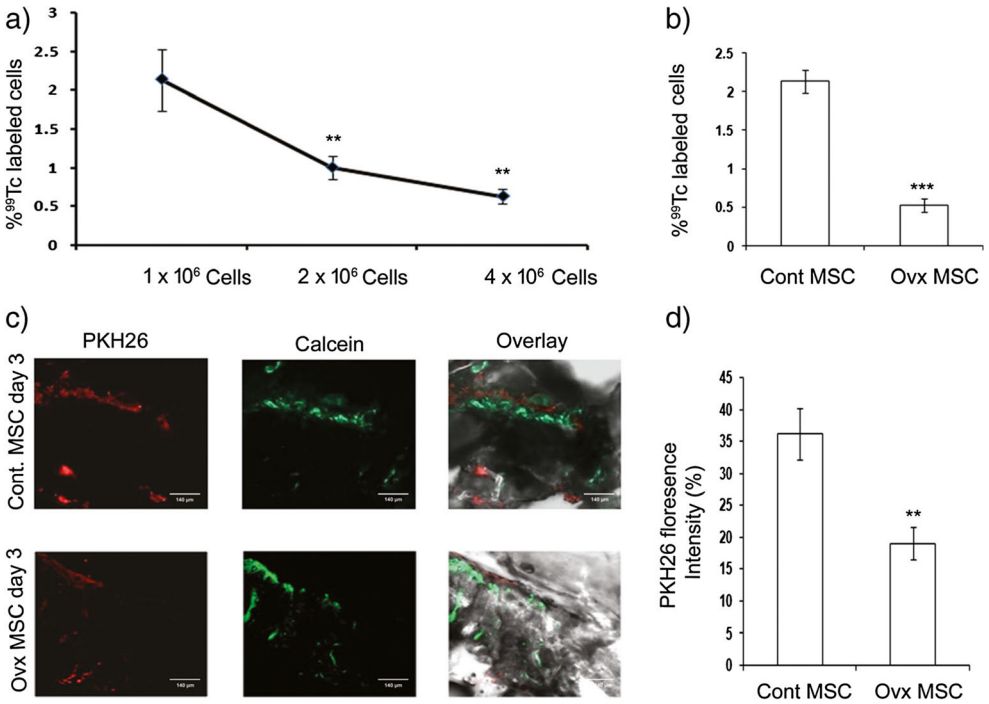

Fig. 4 Diminished migration of Ovx MSC to fracture site compared with control MSC after systemic transplantation. (**a**) SPECT/CT was performed 3 h after systemic transplantation of increasing number of cont ^{99m}Tc-HMPAO-MSC to rats bearing fracture at femur metaphysis. (**b**) Bar diagram indicating reduced counts at the fracture site when Ovx MSC was transplanted compared to cont MSC. Signal at the femur epiphysis drill-hole region of interest (ROI), measured as counts/min was normalized by subtracting the background signal found in an equal ROI in the contralateral unfractured femur. (**c**) Representative photomicrographs of ^{PKH26}MSC, calcein and merged fluorescence in the phase-contrast mode at the fracture site 3 days after systemic transplantation of MSC (magnification 10×). (**d**) Quantification using Carl Zeiss AM 4.2 image-analysis software showed that the fluorescent intensity in the Ovx ^{PKH26}MSC was less than the control ^{PKH26}MSC group. $^{**}p<0.01$ and $^{***}p<0.001$ vs. placebo; $^{\$\$}p<0.01$ and $^{\$\$\$}p<0.001$ and

half-lives. This had additionally allowed us to study the pattern of MSC localization at the fracture site. As shown in Fig. 4c, on day 3, control MSC was clearly visible on one fringe of the fracture and endosteum close to the fracture rim, and alongside labeled cells, localization of calcein label suggested active bone formation. Both control and Ovx MSC had flecked pattern of label. Total fluorescent intensity was less at the fracture site of rats transplanted with Ovx MSC compared to those transplanted with control MSC ($p<0.01$) (Fig. 4d).

Osteoinduction by MSC at the Fracture Site and ER Dependence

Representative confocal imaging of calcein labels at the fracture site of various groups is shown in Fig. 5a. Total calcein binding intensity in the callus of rats treated with control MSC was ~2.0-fold higher ($p<0.001$) and Ovx MSC was 1.4-fold higher ($p<0.05$) than the placebo group (Fig. 5b). Calcein binding in the control MSC was higher than the Ovx MSC group ($p<0.001$). In comparison to placebo group, the ratio of calcein labeled-to-unlabeled area in both control MSC and Ovx MSC was higher than the placebo (placebo vs. control MSC, $p<0.001$ and placebo vs. Ovx MSC $p<0.05$). However, this ratio was higher in cont MSC over Ovx MSC ($p<0.001$) (Fig. 5c), suggesting that osteoinduction activity in the control MSC group was more extensive throughout the callus as compared with Ovx MSC. No difference in the calcein binding parameters was observed when placebo group was compared with control MSC + fluvestrant group (Fig. 5c).

Table 3 Parameters from ^{99m}Tc-HMPAO labeled MSC in rats with fracture

No. of cells injected	Total counts in rats (cpm/mm^2)	Counts at fracture site (cpm/mm^2)	No. of cells at fracture site
1×10^6	510,458±92,378	11,210±3075	21,142±2277
2×10^6	848,455±59,367	7169±1448	16,590±2198
4×10^6	543,337±73,661	3438±546	25,589 ±3332

Data represent the mean ± SEM (n=3 rats/transplantation)

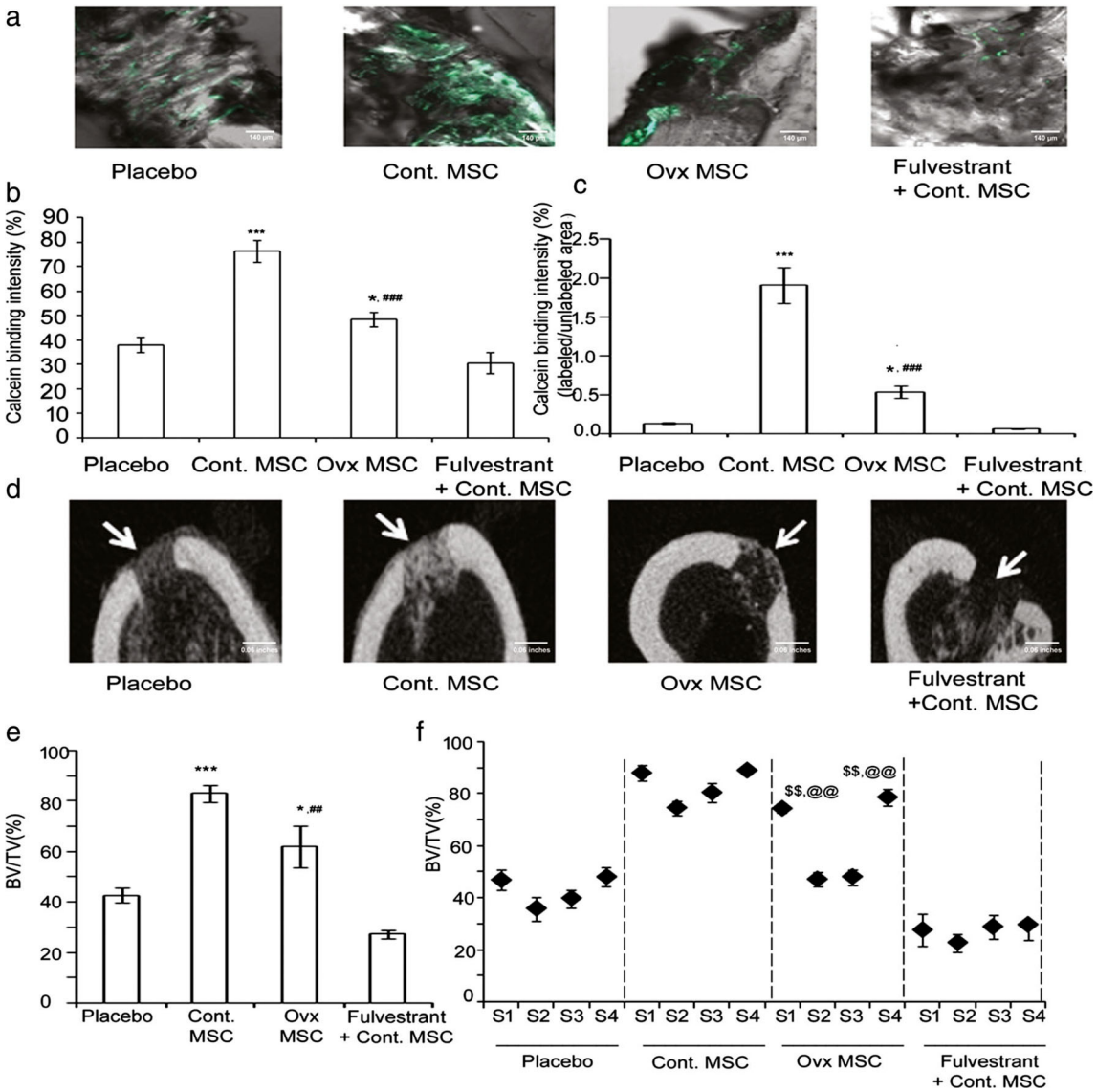

Fig. 5 Diminished osteoinduction and bone regeneration at the fracture by systemically transplanted Ovx MSC compared with cont MSC. (**a**) Representative confocal images (10×) of calcein labeling shown in the callus of drill-hole of various groups after 2 weeks of treatments. (**b**) Quantification of the mean intensity of calcein label per pixel in the entire callus region showing enhanced osteoinduction by cont MSC over other groups. Fulvestrant administration completely mitigated cont MSC induced osteoinduction. (**c**) Calcein labeled area in the callus was also highest in rats transplanted with cont MSC over other treatments. (**d**-) Representative μCT images of the callus in various groups. (**e**) Bone volume/tissue volume (BV/TV, %) was highest in the fracture site of rats transplanted with cont MSC compared to other groups. Ovx MSC transplantation also increased BV/TV over the placebo group. Fulvestrant administration to rats transplanted with cont MSC reduced BV/TV less than placebo group. (**f**) BV/TV of entire callus was divided into four equal areas (segments denoted by S1-S4) and values plotted. All but Ovx MSC group had equal BV/TV in S1-S4. BV/TV varied between different segments of Ovx MSC group. All values are expressed as mean ± SEM ($n=6$); *$p<0.05$, ***$p<0.001$ vs. placebo, $^{\#\#\#}p<0.001$ vs. cont MSC, $^{\$\$}p<0.01$ vs. S2 and $^{@@}p<0.01$ vs. S3

Representative μCT images of femur metaphysis cross-section containing fracture of different groups are shown in Fig. 5d. In comparison to placebo group, bone volume/tissue volume (BV/TV%) determined from μCT in both control and Ovx MSC was higher than the placebo (placebo vs. control MSC, $p<0.001$ and placebo vs. Ovx MSC $p<0.05$) (Fig. 5e). However, this ratio was higher in control MSC over Ovx MSC ($p<0.01$). To determine the uniformity of bone (Fig 5e). BV/TV was not different between the placebo and control MSC + fluvestrant groups (Fig. 5e). To determine the uniformity of bone regeneration at the fracture, we next measured BV/TV in the callus by dividing it into four equal segments (S1-S4). BV/TV values were not different between four segments in placebo, control MSC and control MSC + fluvestrant groups, while these were scattered (significantly different from each other) in the Ovx MSC group, suggesting that bone formation was not uniform in the latter group (Fig. 5f).

Systemic Transplantation of MSC to Ovx Rats and the Effect of E2

We next assessed the effect of transplanting control or Ovx MSC on osteoinduction in Ovx (osteopenic) rats and as shown in Fig. 6, control MSC transplantation had increased calcein binding ($p<0.05$) (Fig. 6a) and bone volume (BV/TV, $p<0.01$) (Fig. 6b) over the placebo group. Calcein binding intensity and BV/TV were not different between the placebo and Ovx MSC groups (Fig. 6a and b). E2 administration to Ovx rats resulted in significant increases in both calcein binding intensity ($p<0.05$) and BV/TV over the Ovx + placebo group ($p<0.01$) (Fig. 6a and b).

Local Application of MSC and Osteoinduction

Because fracture tropism of Ovx MSC after systemic transplant was greatly diminished compared to control MSC, resulting in reduced availability of Ovx MSC at the fracture site, we asked whether the availability Ovx MSC equal in number with cont MSC would result in comparable osteoinduction. We loaded equal number (2×10^4) of control PKH26-MSC and Ovx PKH26-MSC in the scaffold. This number was derived from SPECT/CT calculation of the number of MSC localized at the wound site after systemic transplantation (refer to Table 3). Loading equal number of MSC to the scaffold was further confirmed by confocal microscopy of scaffold followed by densitometry (Fig. 7a). Control rats (ovary intact) were applied with empty scaffold, scaffold with control PKH26-MSC or scaffold with Ovx PKH26-MSC at the fracture site. As shown in Fig. 7b, on day 14, calcium binding in control PKH26-MSC and Ovx PKH26-MSC containing scaffold groups was higher than the rats with empty scaffold at the fracture site (placebo vs. control PKH26-MSC, $p<0.001$ and placebo vs. Ovx PKH26-MSC, $p<0.05$). However, calcein was higher in control PKH26-MSC than Ovx PKH26-MSC ($p<0.05$). As shown in Fig. 7c, BV/TV was higher in control PKH26-MSC containing scaffold as compared with the rats with empty scaffold at the fracture site ($p<0.001$). BV/TV was not different between Ovx PKH26-MSC and empty scaffold group (Fig. 7c).

Discussion

Here, we studied alterations that take place in MSC in response to prolonged E2 deficiency, particularly with respect to enhancement of fracture healing. Our major findings include, i) MSC population in the BM of Ovx rats was substantially diminished and doubling time was ~70 % longer compared to ovary intact (control) group, ii) fracture tropism of Ovx MSC was only 25 % of the control MSC, iii) osteoinduction at the fracture sites of control and Ovx rats were lesser achieved by Ovx MSC than control MSC, iv) osteoinduction pattern at the fracture site by Ovx MSC was non-uniform in contrast to uniform induction by control MSC, v) equal number of MSC when applied to the fracture site resulted in significantly lower osteoinduction by Ovx MSC compared to control MSC and vi) anti-estrogen, fulvestrant administration to control rats abolished fracture healing ability of control MSC. These findings define several functional anomalies in BM-MSCs from rats with osteopenia that could negatively affect fracture healing.

Age-related decline in the number of MSC in the bone marrow has been observed in rodents and humans [38, 39].

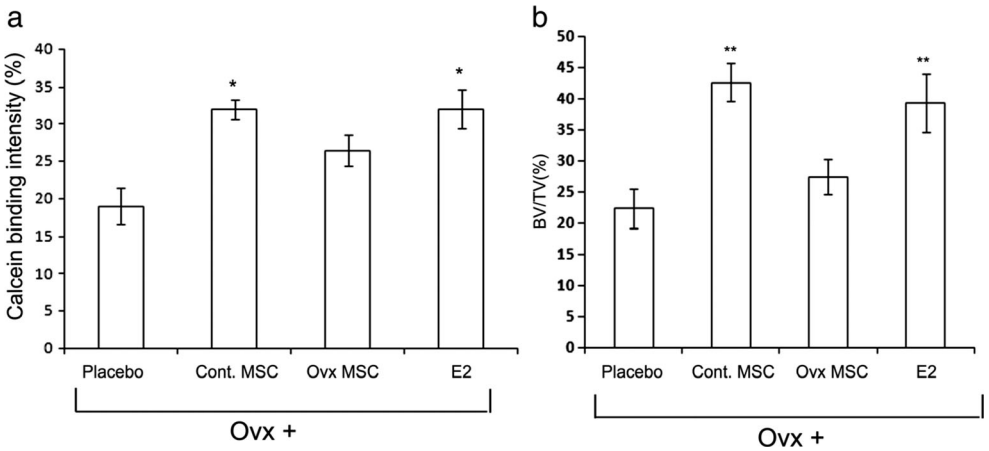

Fig. 6 Lack of osteoinduction and bone generation by systemically transplanted Ovx MSC at the fracture site of osteopenic rats. Cont MSC or Ovx MSC (each 1×10^6 cells) was systemically transplanted to Ovx rats. E2 dose was 60 μg/kg/d, s.c. After 14 days of various treatments, (**a**) calcein binding intensity at the callus was greater in the cont MSC and E2 treated groups over the placebo and Ovx MSC groups and (**b**) BV/TV was increased in the control MSC and E2 treated groups compared to the placebo and Ovx MSC groups. All values are expressed as mean ± SEM ($n=5$); *$p<0.05$, **$p<0.01$, ***$p<0.001$

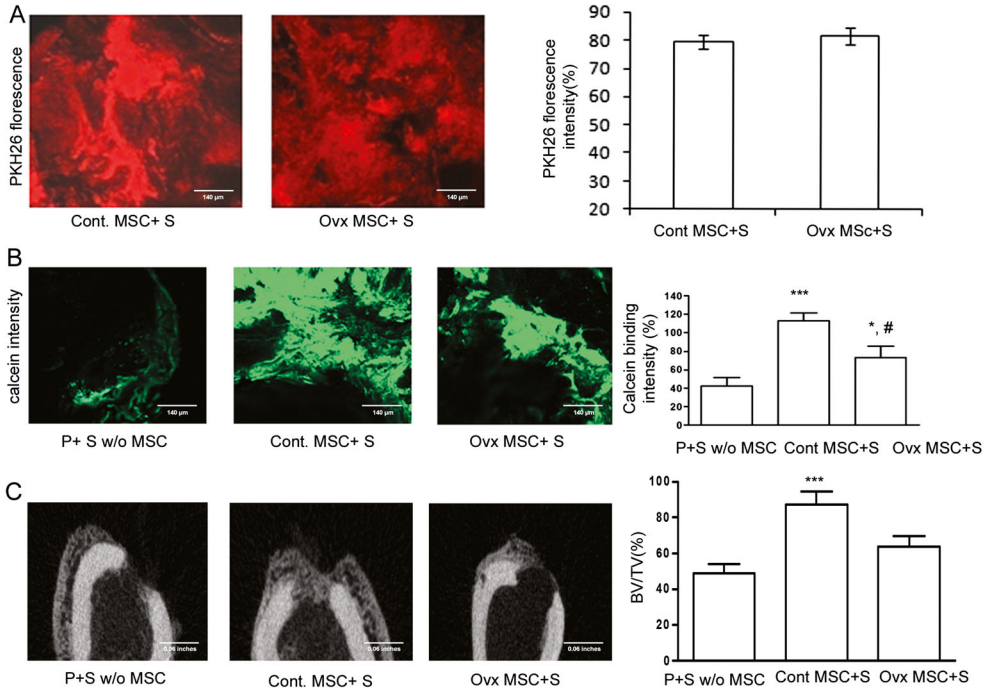

Fig. 7 Diminished osteoinduction and bone regeneration by local transplantation of Ovx MSC at the fracture site of ovary intact adult rats compared with cont MSC. (**a**) control ^{PKH26}MSC or Ovx ^{PKH26}MSC (3×10^4 cells) were loaded in n-HA/gel/CMC scaffold construct and photographed (10×) and (**b**) fluorescent intensity determined which showed comparable values between the two groups. (**c**) Representative photomicrograph of calcein labeled callus after 14 days. (**d**) Quantification of the mean intensity of calcein label per pixel in the entire callus region showing enhanced osteoinduction by cont ^{PKH26}MSC over other groups. (**e**) Representative μCT images of the callus in various groups and (**f**) quantification of BV/TV showed greater bone volume in cont ^{PKH26}MSC group over Ovx ^{PKH26}MSC. All values are expressed as mean ± SEM (n=5); *p<0.05, ***p<0.001 vs. P + S w/o MSC, $^{\#}p$<0.05 vs. Cont MSC+S. P = placebo, S = scaffold, w/o = without

There was a marked depletion of MSC in the BM of Ovx rats that was accompanied by a prolongation of doubling time (delayed renewal process) compared with the sham group thus suggesting that in fact the precursor source of stromal cell population was diminished in the Ovx rats. Further, we found increase in adipogenesis and diminished osteogenesis in Ovx MSC in comparison to control MSC. Our findings supported that of Rodriguez et al. where BM MSC derived from post-menopausal osteoporotic individuals showed reduced osteogenic and increased adipogenic differentiation [40] but differed from that reported by Ying et al. where a mixed population of BM cells showed increase in both osteogenesis and adipogenesis [41]. Furthermore, our data showed that Ovx MSC were refractory to E2 treatment with respect to osteogenic differentiation as E2 did not stimulate osteogenesis in these but did so in control MSC. Loss of E2 response in the Ovx MSC may be a consequence of altered ER co-activator/repressor balance occurring as a result of long-term E2 deficiency and/or the epigenetic changes that are known to regulate E2 signaling in breast cancer cells [42]. Presently, we have no definitive answer to the cause of insensitivity of Ovx MSC to E2.

Reduced MSC population in the Ovx rats could be due to apoptosis as E2 at a pharmacological concentration (10^{-7} M) has been shown to exert anti-apoptotic/prosurvival effect on MSC in vitro [43]. In postmenopausal women, osteoporosis delays fracture healing and causes reduced bone deposition [44], and together, the recovery of functional competence of the fractured bone in osteoporotic women is delayed [22]. Given that MSC triggers fracture healing, a severely reduced number and proliferative capacity of MSC in addition to impaired ability to differentiate to osteoblasts could underlie the attenuated healing ability of fractures in women deficient in E2. Because, we used rats that were young adults, Ovx under this setting resembled more with E2 deficiency-induced osteopenia in young women such as those suffering from HA or anorexia [2] than post-menopausal women.

Although, E2 is not a recommended treatment for fracture healing, a recent study showed improvement in fracture healing based on histological and biomechanical parameters in Ovx rats treated with E2, thus suggesting a positive role of the hormone in promoting fracture healing [43]. However, the reported study used a prophylactic design where E2 treatment was given to rats soon after Ovx without allowing the time for osteopenia to develop. Our finding that osteoinduction was deficient in Ovx rats that were osteopenic further supports the thesis that E2 could positively impact fracture healing. In addition, we showed that pharmacological blockade of ER in ovary intact rats by fulvestrant completely abrogated cont MSC-induced osteoinduction at the fracture site, suggesting

that bone regenerative capacity of MSC required functional ER signaling.

SPECT/CT data using ^{99m}Tc-HMPAO labelled cells showed that fracture tropism of Ovx MSC is 1/4th of control MSC in ovary intact rats. Estimated migration of control MSC in our study was 2.0 % whereas luciferase expressing mouse BM-MSC transplanted to transgenic mice (CMV-R26R or BMP-2-Lac Z) that bore tibial fracture reported a homing efficiency of ~1 % [13]. The difference in the percentage of MSC migration to fracture site between our and the reported study could stem from the variation in the animals used (outbred rat by us and inbred transgenic mice in the report) and the sensitivity of the detection methods (scintigraphy by us and bioluminescence imaging in the report). However, from both studies, it appears that the migration of systemically transplanted MSC to the fracture site is only a very tiny fraction of the total and the major retention sites of MSC are lung and the reticulo-endothelial bed. In addition, our data showed that MSC number at the fracture site did not increase beyond 2.0 % of injected MSC suggesting that with systemic transplantation, 2.0 % MSC homing to the fracture site was maximally achieved with control MSC and 0.4 % with Ovx MSC.

From the PKH26 labeling experiment, transplanted control MSC at day 3 was found to be localized as a stripe on the inner surface of the fracture defect and, juxtaposing MSC, an intense calcein labeling was observed, which appeared to serve as a focal point for bone regeneration. At day 14, unlike the uniform calcein labeling observed upon transplantation of control MSC or in placebo group, Ovx MSC had uneven labeling pattern. This observation suggested that Ovx MSC while migrated much less than the control MSC to the fracture site, in addition had spatially impaired osteoinduction response that did not cover the complete fracture area and thus could lead to unequal and defective bone regeneration. Indeed, μCT data supported this hypothesis as BV/TV at different locations of callus in Ovx MSC group varied significantly from each other whilst it remained similar in control MSC or placebo group, suggesting that Ovx MSC produced irregular as opposed to uniform bone regeneration by control MSC. The underlying reason for the failure to stimulate even regeneration of bone at the fracture site by Ovx MSC needs future studies. Furthermore, whether such irregularly deposited bone could impact biomechanical competence remains to be assessed however direct measurement of resistance to compression failure in the drill-hole fracture model cannot be undertaken and instead requires indirect measurement by finite element analysis of μCT data.

Because fracture homing by Ovx MSC was less than the control MSC, the possibility that diminished osteoinduction by the former was actually contributed by decreased homing arose. To answer this question, we applied equal number of control or Ovx MSC to the fracture site of ovary intact rats using a scaffold and observed significantly reduced osteoinduction by Ovx MSC compared to control MSC, thus suggesting that bone regenerative ability of Ovx MSC was impaired. These data suggest that Ovx MSC has reduced ability to migrate to the fractured site as well as bone regeneration. E2 is known to regulate expression of various chemokines and their signaling in normal [45] and malignant cells [46]. Out of these, monocyte/macrophage chemoattractant protein-1 (MCP-1) and stromal cell-derived factor-1 alpha (SDF-1α) have been shown to be modulated by E2 in MSC [47]. Future studies addressing whether or not E2 modulated MCP-1 and SDF-1α in MSC to regulate fracture tropism would be important. Osteoinduction by control MSC was completely abolished by fluvestrant which suggested that ER signaling in MSC was essential for this effect. Thus, reduced migration and osteoinduction by Ovx MSC in ovary intact rats suggested possible alterations in ER signaling apparatus in these cells, which could be addressed in future studies.

Although in E2-replete rats, the osteoinductive effect of Ovx MSC was lower than control MSC, it was still greater than the placebo group. On the other hand, in osteopenic rats, Ovx MSC did not exhibit osteoinduction while control MSC did. This result imply that autologous BM-MSC from subjects with prolonged E2-deficiency as in the case of postmenopausal osteoporotics may not be effective in promoting fracture healing but that from E2-replete subjects could be.

There are a few caveats in this study. First, we have not checked the status of ER and the associated signaling machinery in Ovx MSC that could be responsible for reduced E2-induced osteogenic differentiation. Second, as bone regeneration at the fracture site was stimulated by control MSC in Ovx rats, it suggested that systemic E2 may not have a role in osteoinduction by MSC. On the other hand, fulvestrant attenuated osteoinduction by control MSC in E2-replete condition. These two apparently conflicting observations from two different in vivo systems remain unaddressed. Third, we have not compared the efficacy of MSC-induced bone regeneration with osteogenic therapy such as PTH [48] and local application of rhBMP-2 [49] which is approved by US FDA for enhanced bone healing. Fourth, we have not extended the study to cover the remodeling stage in which the healing bone is restored to its original shape, structure, and mechanical strength.

In conclusion, we showed that osteopenia induced by prolonged E2 deficiency severely depletes BM-MSC, impairs their growth ability, decreases homing ability to the fracture site, reduces osteoinduction efficacy and displays anomalous pattern of bone regeneration at the fractured callus. Our preclinical data also suggests that MSC from individuals suffering from postmenopausal osteoporosis may not be effective in improving fracture healing in an autologous setting.

Acknowledgments The authors are thankful for the technical assistance provided by Kavita Singh at the Confocal Microscopy Facility, SAIF division, CSIR-CDRI.

Conflict of Interest Although in no way related to this study, NC has received research support from GlaxoSmithKline Consumer Health Care, Gurgaon, India and served as an advisory board member of Alkem Laboratories Ltd, India. All other authors have no conflict of interest.

Funding Authors acknowledge funding from Council of Scientific and Industrial Research (CSIR) to [N.C.] (BSC0201, ASTHI); Research fellowship grants from the Department of Biotechnology [DT], Indian Council of Medical Research [MPK] and CSIR (S.P.C).

Supporting grants Council of Scientific and Industrial Research, Indian Council of Medical Research and Department of Biotechnology, Government of India.

References

1. Gruber, R., Koch, H., Doll, B. A., Tegtmeier, F., Einhorn, T. A., & Hollinger, J. O. (2006). Fracture healing in the elderly patient. *Experimental Gerontology, 41*(11), 1080–1093.
2. Elford K., & Claman P., (2004). Osteoporosis in reproductive age women: Impact of sex steroid replacement. *Encyclopedia of Endocrine Diseases*, pp. 441–446
3. Balasch, J. (2003). Sex steroids and bone: current perspectives. *Human Reproduction Update, 9*(3), 207–222.
4. Bethel, M., Chitteti, B. R., Srour, E. F., & Kacena, M. A. (2013). The changing balance between osteoblastogenesis and adipogenesis in aging and its impact on hematopoiesis. *Current Osteoporosis Reports, 11*(2), 99–106.
5. Arrabal, P. M., Visser, R., Santos-Ruiz, L., Becerra, J., & Cifuentes, M. (2013). Osteogenic molecules for clinical applications: improving the BMP-collagen system. *Biological Research, 46*(4), 421–429.
6. Nevins, M. L., & Reynolds, M. A. (2011). Tissue engineering with recombinant human platelet-derived growth factor BB for implant site development. *Compendium of Continuing Education in Dentistry, 32*(2), 18. 20–7.
7. Oryan, A., Alidadi, S., Moshiri, A., & Maffulli, N. (2014). Bone regenerative medicine: classic options, novel strategies, and future directions. *Journal of Orthopaedic Surgery and Research, 9*(1), 18. doi:10.1186/1749-799X-9-18.
8. Liebergall, M., Schroeder, J., Mosheiff, R., et al. (2013). Stem cell-based therapy for prevention of delayed fracture union: a randomized and prospective preliminary study. *Molecular Therapy, 21*(8), 1631–1638.
9. Frohlich, M., Grayson, W. L., Wan, L. Q., Marolt, D., Drobnic, M., & Vunjak-Novakovic, G. (2008). Tissue engineered bone grafts: biological requirements, tissue culture and clinical relevance. *Current Stem Cell Research & Therapy, 3*(4), 254–264.
10. Kean, T. J., Lin, P., Caplan, A. I., & Dennis, J. E. (2013). MSCs: Delivery routes and engraftment, cell-targeting strategies, and immune modulation. *Stem Cells International*. doi:10.1155/2013/732742.
11. Horwitz, E. M., Gordon, P. L., Koo, W. K., et al. (2002). Isolated allogeneic bone marrow-derived mesenchymal cells engraft and stimulate growth in children with osteogenesis imperfecta: Implications for cell therapy of bone. *Proceedings of the National Academy of Sciences of the United States of America, 99*(13), 8932–8937.
12. Alm, J. J., Koivu, H. M., Heino, T. J., Hentunen, T. A., Laitinen, S., & Aro, H. T. (2010). Circulating plastic adherent mesenchymal stem cells in aged hip fracture patients. *Journal of Orthopaedic Research, 28*(12), 1634–1642.
13. Granero-Molto, F., Weis, J. A., Miga, M. I., et al. (2009). Regenerative effects of transplanted mesenchymal stem cells in fracture healing. *Stem Cells, 27*(8), 1887–1898.
14. Shirley, D., Marsh, D., Jordan, G., McQuaid, S., & Li, G. (2005). Systemic recruitment of osteoblastic cells in fracture healing. *Journal of Orthopaedic Research, 23*(5), 1013–1021.
15. Kolios, L., Hoerster, A. K., Sehmisch, S., et al. (2010). Do estrogen and alendronate improve metaphyseal fracture healing when applied as osteoporosis prophylaxis? *Calcified Tissue International, 86*(1), 23–32.
16. Westerlind, K. C., Wronski, T. J., Ritman, E. L., et al. (1997). Estrogen regulates the rate of bone turnover but bone balance in ovariectomized rats is modulated by prevailing mechanical strain. *Proceedings of the National Academy of Sciences of the United States of America, 94*(8), 4199–4204.
17. Squire, M., Brazin, A., Keng, Y., & Judex, S. (2008). Baseline bone morphometry and cellular activity modulate the degree of bone loss in the appendicular skeleton during disuse. *Bone, 42*(2), 341–349.
18. Carod Artal, F. J. (1995). What should first be considered in the treatment of epileptic patients: control of seizures or quality of life? *Revista de Neurologia, 23*(124), 1325.
19. McCann, R. M., Colleary, G., Geddis, C., et al. (2008). Effect of osteoporosis on bone mineral density and fracture repair in a rat femoral fracture model. *Journal of Orthopaedic Research, 26*(3), 384–393.
20. Hao, Y. J., Zhang, G., Wang, Y. S., et al. (2007). Changes of microstructure and mineralized tissue in the middle and late phase of osteoporotic fracture healing in rats. *Bone, 41*(4), 631–638.
21. Augat P., Simon U., Liedert A., Claes L., (2005). Mechanics and mechano-biology of fracture healing in normal and osteoporotic bone. *Osteoporosis International*, Suppl 2:S36-S43
22. Barrios, C., Brostrom, L. A., Stark, A., & Walheim, G. (1993). Healing complications after internal fixation of trochanteric hip fractures: the prognostic value of osteoporosis. *Journal of Orthopaedic Trauma, 7*(5), 438–442.
23. Hong, L., Zhang, G., Sultana, H., Yu, Y., & Wei, Z. (2011). The effects of 17-beta estradiol on enhancing proliferation of human bone marrow mesenchymal stromal cells in vitro. *Stem Cells and Development, 20*(5), 925–931.
24. Turner, R. T., Riggs, B. L., & Spelsberg, T. C. (1994). Skeletal effects of estrogen. *Endocrine Reviews, 15*(3), 275–300.
25. Zhang, L., & Chan, C. (2010). Isolation and enrichment of rat mesenchymal stem cells (MSCs) and separation of single-colony derived MSCs. *Journal of Visualized Experiments*. doi:10.3791/1852.
26. Gruber, H. E., Somayaji, S., Riley, F., et al. (2012). Human adipose-derived mesenchymal stem cells: serial passaging, doubling time and cell senescence. *Biotechnic & Histochemistry, 87*(4), 303–311.
27. Bhargavan, B., Gautam, A. K., Singh, D., et al. (2009). Methoxylated isoflavones, cajanin and isoformononetin, have non-estrogenic bone forming effect via differential mitogen activated protein kinase (MAPK) signaling. *Journal of Cellular Biochemistry, 108*(2), 388–399. doi:10.1002/jcb.22264.
28. Swarnkar, G., Sharan, K., Siddiqui, J. A., et al. (2011). A novel flavonoid isolated from the steam-bark of Ulmus wallichiana planchon stimulates osteoblast function and inhibits osteoclast and adipocyte differentiation. *European Journal of Pharmacology, 658*(2–3), 65–73.
29. Khan, K., Sharan, K., Swarnkar, G., et al. (2013). Positive skeletal effects of cladrin, a naturally occurring dimethoxydaidzein, in osteopenic rats that were maintained after treatment discontinuation. *Osteoporosis International, 24*, 1455–1470. doi:10.1007/s00198-012-2121-8.
30. Abbas, S., Khan, K., Khan, M. P., et al. (2013). Developmental exposure to As, Cd, and Pb mixture diminishes skeletal growth and

causes osteopenia at maturity via osteoblast and chondrocyte malfunctioning in female rats. *Toxicological Sciences, 134*(1), 207–220.
31. Ngueguim, F. T., Khan, M. P., Donfack, J. H., et al. (2012). Evaluation of Cameroonian plants towards experimental bone regeneration. *Journal of Ethnopharmacology, 141*(1), 331–337.
32. de Vries, E. F., Roca, M., Jamar, F., Israel, O., & Signore, A. (2010). Guidelines for the labelling of leucocytes with (99 m)Tc-HMPAO. Inflammation/Infection Taskgroup of the European Association of Nuclear Medicine. *European Journal of Nuclear Medicine and Molecular Imaging, 37*(4), 842–848.
33. Sharan, K., Mishra, J. S., Swarnkar, G., et al. (2011). A novel quercetin analogue from a medicinal plant promotes peak bone mass achievement and bone healing after injury and exerts an anabolic effect on osteoporotic bone: the role of aryl hydrocarbon receptor as a mediator of osteogenic action. *Journal of Bone and Mineral Research, 26*(9), 2096–2111.
34. Hildebrand, T., & Ruegsegger, P. (1997). Quantification of bone microarchitecture with the structure model index. *Computer Methods in Biomechanics and Biomedical Engineering, 1*(1), 15–23.
35. Sagar, N., Soni, V. P., & Bellare, J. R. (2012). Influence of carboxymethyl chitin on stability and biocompatibility of 3D nanohydroxyapatite/gelatin/carboxymethyl chitin composite for bone tissue engineering. *Journal of Biomedical Materials Research, 100*(3), 624–636.
36. Sagar, N., Pandey, A. K., Gurbani, D., et al. (2013). In-vivo efficacy of compliant 3D nano-composite in critical-size bone defect repair: a six month preclinical study in rabbit. *PLoS ONE, 8*, e77578. doi:10.1371/journal.pone.0077578.
37. Rai, R. K., Barbhuyan, T., Singh, C., et al. (2013). Total water, phosphorus relaxation and interatomic organic to inorganic interface are new determinants of trabecular bone integrity. *PLoS ONE, 8*(12), e83478. doi:10.1371/journal.pone.0083478.
38. Stenderup, K., Justesen, J., Clausen, C., & Kassem, M. (2003). Aging is associated with decreased maximal life span and accelerated senescence of bone marrow stromal cells. *Bone, 33*(6), 919–926.
39. Wilson, A., Shehadeh, L. A., Yu, H., & Webster, K. A. (2010). Age-related molecular genetic changes of murine bone marrow mesenchymal stem cells. *BMC Genomics, 11*, 229. doi:10.1186/1471-2164-11-229.
40. Rodriguez, J. P., Montecinos, L., Rios, S., et al. (2000). Mesenchymal stem cells from osteoporotic patients produce a type I collagen-deficient extracellular matrix favoring adipogenic differentiation. *Journal of Cellular Biochemistry, 79*(4), 557–565.
41. Gao, Y., Jiao, Y., Nie, W., et al. (2014). In vitro proliferation and differentiation potential of bone marrow-derived mesenchymal stem cells from ovariectomized rats. *Tissue and Cell, S0040–8166*(14), 00075–5.
42. Hervouet, E., Cartron, P. F., Jouvenot, M., & Delage-Mourroux, R. (2013). Epigenetic regulation of estrogen signaling in breast cancer. *Epigenetics, 8*(3), 237–245. doi:10.4161/epi.23790.
43. Ayaloglu-Butun, F., Terzioglu-Kara, E., Tokcaer-Keskin, Z., & Akcali, K. C. (2012). The effect of estrogen on bone marrow-derived rat mesenchymal stem cell maintenance: inhibiting apoptosis through the expression of Bcl-xL and Bcl-2. *Stem Cell Reviews and Reports, 8*(2), 393–401. doi:10.1007/s12015-011-9292-0.
44. Diwan, A. D., Leong, A., Appleyard, R., Bhargav, D., Fang, Z. M., & Wei, A. (2013). Bone morphogenetic protein-7 accelerates fracture healing in osteoporotic rats. *Indian Journal of Orthopaedics, 47*(6), 540–546.
45. Nebel, D., Jönsson, D., Norderyd, O., Bratthall, G., & Nilsson, B. O. (2010). Differential regulation of chemokine expression by estrogen in human periodontal ligament cells. *Journal of Periodontal Research, 45*(6), 796–802. doi:10.1111/j.1600-0765.2010.01308.x.
46. Boudot, A., Kerdivel, G., Habauzit, D., et al. (2011). Differential estrogen-regulation of CXCL12 chemokine receptors, CXCR4 and CXCR7, contributes to the growth effect of estrogens in breast cancer cells. *PLoS ONE, 6*(6), e20898. doi:10.1371/journal.pone.0020898.
47. Ji, J. F., He, B. P., Dheen, S. T., & Tay, S. S. (2004). Interactions of chemokines and chemokine receptors mediate the migration of mesenchymal stem cells to the impaired site in the brain after hypoglossal nerve injury. *Stem Cells, 22*(3), 415–427.
48. Neer, R. M., Arnaud, C. D., Zanchetta, J. R., et al. (2001). Effect of parathyroid hormone (1–34) on fractures and bone mineral density in postmenopausal women with osteoporosis. *The New England Journal of Medicine, 344*(19), 1434–1441.
49. Valentin-Opran, A., Wozney, J., Csimma, C., Lilly, L., & Riedel, G. E. (2002). Clinical evaluation of recombinant human bone morphogenetic protein-2. *Clinical Orthopaedics and Related Research, 2*(395), 110–120.